Bioprocess and Biosystems Engineering (2022) 45:2043–2060
https://doi.org/10.1007/s00449-022-02808-7

RESEARCH PAPER

A multi-component approach for co-immobilization of lipases on silica-coated magnetic nanoparticles: improving biodiesel production from waste cooking oil

Narges Alikhani[1] · Mansour Shahedi[1] · Zohreh Habibi[1] · Maryam Yousefi[2] · Saba Ghasemi[3] · Mehdi Mohammadi[4]

Received: 31 May 2022 / Accepted: 24 October 2022 / Published online: 10 November 2022

Abstract

The capability of multi-component reactions in rapid immobilization of enzymes was considered for co-immobilization of *Thermomyces lanuginous* lipase (TLL) and *Candida antarctica* lipase B (CALB) [TLL: CALB]; *Rhizomucor miehei* lipase (RML) and CALB [RML: CALB] on amine-functionalized silica-coated magnetic nanoparticles (Fe_3O_4@SiO_2-NH_2). Immobilization of different ratios of lipases was performed within 3 h under mild conditions; producing specific activity ranging from 29 to 35 U/mg for TLL:CALB and 21–34 U/mg for RML:CALB. The co-immobilized derivatives showed improved co-solvent and thermal stability compared to the corresponding free enzymes. All the derivatives were also used to catalyze the transesterification of waste cooking oil with methanol to produce biodiesel (fatty acid methyl esters). Response surface method (RSM) and a central composite rotatable design (CCRD) were used to study the effects of different factors on the FAME yield. Fe_3O_4@SiO_2-NH_2-RML-CALB and Fe_3O_4@SiO_2-NH_2-TLL-CALB had maximum FAME yields of 99–80%, respectively.

Keywords Biodiesel · Co-immobilization · Magnetic nanoparticles · Multi-component reaction · Lipase

Introduction

Fossil fuels have been used for many years as the most dominant fuel for motor engines. However, the serious crisis of declining fossil fuel resources and environmental pollution have led to a search for new renewable biofuels and finding novel alternative fuel sources [1]. Mono alkyl esters of long-chain fatty acids, known as biodiesel, has been suggested as one of promising renewable fuels. Biodiesel can be produced through transesterification of various oils and fats via alcoholysis of triglyceride [2]. The transesterification reaction performs through a catalytic pathway. The catalyst may be alkaline [3], acid [4, 5], or enzyme [6–8]. Enzyme catalyzed reactions are environmentally friendly, and require mild reaction conditions and compatible with a wide variety of feedstocks [9].

Lipases have the ability to catalyze a wide range of reactions such as esterification, transesterification, and polymerization with high chemo-, regio- and stereoselectivity [10]. Free enzymes are cheaper than immobilized lipases, but they are often easily inactivated and difficult to be separated from the reaction system [11]. Immobilization of lipases giving rise to high operational stability and reusability makes them suitable for batch or continuous systems.

Lipases can be immobilized on various supports by several methods like adsorption, cross-linking, covalent attachment, and physical entrapment [12]. The covalent attachment of an enzyme on a solid support for irreversible enzyme immobilization is usually preferred when leaching of an enzyme from the support is the main concern [13]. However, there are some disadvantages in covalent binding

✉ Zohreh Habibi
Z_habibi@sbu.ac.ir

✉ Maryam Yousefi
M.yousefi@avicenna.ac.ir

[1] Department of Organic Chemistry and Oil, Faculty of Chemistry, Shahid Beheshti University, Tehran, Iran

[2] Nanobiotechnology Research Center, Avicenna Research Institute, ACECR, Tehran, Iran

[3] Department of Chemistry, Ilam Branch, Islamic Azad University, Ilam, Iran

[4] Bioprocess Engineering Department, Institute of Industrial and Environmental Biotechnology, National Institute of Genetic Engineering and Biotechnology (NIGEB), Tehran, Iran

of enzymes; for example, the conditions for attachment are more complicated compared to the other methods such as physical adsorption and ionic binding. Factors that are significant in selecting the immobilization strategy are the simplicity of the method, good catalytic activity, immobilization time, stability, and reusability of the immobilized enzyme [14].

There are a wide variety of carriers for lipase immobilization. Magnetic nanoparticles have been identified as a suitable support for stabilization of biological macromolecules [15, 16]. Low toxicity, surface modifiability, and high immobilization capacity also make this type of support an ideal one for enzyme immobilization [17].

Meanwhile, different protocols for immobilization may lead to various properties of a unique enzyme. Recently, new strategies for the covalent binding of enzymes have been developed using isocyanide-based multi-component reactions (ICMRs). The results of using three- and four-component reaction for covalent attachment of enzymes on epoxy, acid, amine, and aldehyde functionalized supports have been reported by our group [18–21].

This simple protocol provides high immobilization yields and loading capacity in a very short reaction time. In traditional immobilization method loading of 10 mg of enzyme on 1 gr of the support takes 24 h of reaction time and this is challenging where the high immobilization capacity is required [22–24]. Furthermore, due to non-quantitative co-immobilization of the used enzymes, it is impossible to calculate the exact amount of each enzyme loaded on the support. While in the ICMRs' method, high loading capacity of the method permits to use high concentration of enzymes for co-immobilization and, most importantly, one can be sure that 100% of each enzyme is immobilized on the support. This is very important when using different ratios of enzymes. The other important point is that each active group on the support offers a unique immobilization protocol which is basically different with other functional groups. For example, with amine group on the surface of support (present study), we deliberately targeted the carboxylic acid groups of the enzyme surface to be involved in the coupling reaction.

Due to great achievement of this protocol, we here describe the use of multi-component reaction for one-pot co-immobilization of lipases on amine-functionalized silica-coated magnetic nanoparticles (Fe_3O_4@SiO_2-NH_2), *Candida antarctica* lipase B (CALB) as a non-specific enzyme was co-immobilized with *Thermomyces lanuginous* lipase (TLL) and *Rhizomucor miehei* Lipase (RML) as 1,3-specific lipases and the effect of the used protocol on functional properties of immobilized lipases was evaluated.

We have recently reported immobilization of CALB, TLL, and RML individually on the amine-functionalized silica-coated magnetic nanoparticles (Fe_3O_4@SiO_2-NH_2) individually. Our results indicated that for immobilized RML, TLL, and CALB (with exactly the same method for immobilization), the maximum fatty acid methyl ester)FAME(yields were approximately low 61, 62, and 52%, respectively [25]. In this report, the time of reaction was lowered from 96 to 72 h by combination of these enzymes and reaching to maximum yields of 99–80% for RML-CALB and TLL-CALB systems, respectively. Until now, different methods have been used for the simultaneous use of two lipase enzymes for biodiesel production. For example, combi-lipase has been proposed as a solution for the simultaneous use of two enzymes. Alves and co-workers reported commercially individually immobilized CALB (Novozym 435) was the less active one (40% conversion after 72 h), individually immobilized RML (Lipozyme RM-IM) and TLL(Lipozyme TL-IM) resulted to 45 and 50% conversion, respectively, but the combination of 80% of RML and 20% of CALB was the best biocatalyst (80% conversion after 25 h) [26]. Poppe and co-workers reported the enzymatic transesterification of olive and palm oils, using standalone or mixtures of three commercially immobilized lipases same as Alves as biocatalysts: Novozym 435 (CALB), Lipozyme TL-IM (TLL), and Lipozyme RM-IM (RML). For olive oil, the combination of 29.0% of TLL, 12.5% of RML, and 58.5% of CALB was the best, allowing for 95% conversion efficiency in 18 h of reaction, up from 50% for the best individual lipase (CALB), and for palm oil, the best enzyme combination was 52.5% of TLL and 47.5% of RML, resulting in 80% of conversion of ethyl esters in 18 h, compared to only 44% when TLL was used as single enzyme [27].

Conversion yields in present work are higher than most of combi-lipase systems also, because in this report, magnetic nanoparticles are used as a carrier, it is much easier to separate the catalyst from the reaction mixture, and it can be embedded with a magnet.

A 5-level-5-factor central composite design (CCD) was then used to design the experiments for biodiesel production using immobilized derivatives and response surface methodology (RSM) was carried out for the procedure of optimization. Several reaction parameters that influence fatty acid methyl ester (FAME) yield reaction, such as temperature, biocatalyst/oil ratio, *t*-butanol concentration, water/oil ratio (for TLL:CALB), water-absorbent/oil (for RML:CALB), and RML:CALB or TLL:CALB ratio, were optimized. The relationship between the parameters and the responses were further analyzed.

Experimental

Materials

Waste cooking oil was purchased from a local restaurant. The molecular weight of the waste cooking oil was found to

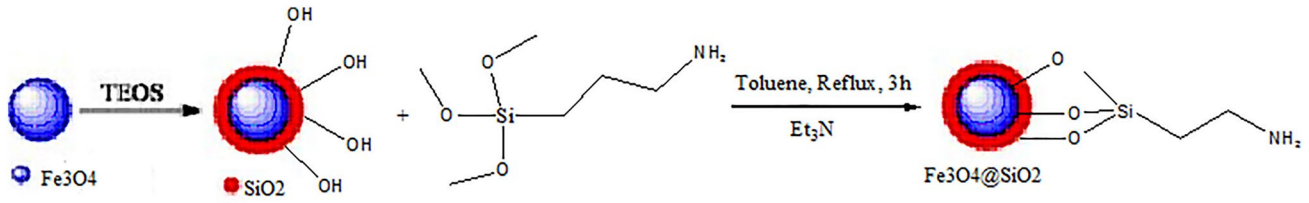

Scheme 1 Functionalization of Fe3O4@SiO2s

be 856.3 g/mol from the saponification value of 196.2 mg KOH/g. The acid value was 76 mg KOH/g. The fatty acid composition of the waste cooking oil was 40.6% oleic acid, 17.6% linoleic acid, 32.2% palmitic acid, and 5.2% stearic acid. Carl Fisher titration method was used to measure the water content in the oil and was determined to be 0.01 (wt.%). Lipase from *Rhizomucor meihei* (RML), *Thermomyces lanuginous* lipase (TLL), $FeCl_2.4H_2O$, $FeCl_3.6H_2O$, triethylamine (Et_3N), *p*-nitrophenyl butyrate (*p*-NPB), and tetraethyl orthosilicate (TEOS) were from Sigma, and *Candida antarctica* lipase B (CALB) was a kind gift from Novoenzymes. Methanol, ethanol, 1-propanol, *t*-butanol, blue silica gel, *n*-hexane, toluene, and cyclohexyl isocyanide were purchased from Merck. 3-(Aminopropyl) trimethoxysilane (APTMS) 97% was purchased from Alfa Aesar.

Methods

Preparation of magnetic nanoparticles (MNPs) and silica-coated magnetic nanoparticles (Fe_3O_4@SiO_2)

Magnetic nanoparticles was prepared by co-precipitation method [28]. 1.25 g of $FeCl_2.4H_2O$ and 3.4 g of $FeCl_3.6H_2O$ in 100 mL deionized water, followed by addition of 9 mL of ammonia solution 32% under vigorous stirring at room temperature for 1 h. The mixture was first washed with distilled water and then with ethanol. The classical Stöber [29] method was used for coating the resulting magnetic nanoparticles with a silica shell. 1 g of Fe_3O_4 was mixed with 80 mL of ethanol. This suspension was dispersed under ultra-sonication for 1 h. Afterwards, in the presence of a constant N_2 gas flux, 20 mL of deionized water and 15 mL of ammonium hydroxide solution were added to the suspension at room temperature followed by adding 3.97 mL of TEOS. The mixture was stirred for 5 h to obtain silica-coated Fe_3O_4 nanoparticles which were washed several times with distilled water and ethanol and were dried at room temperature.

Functionalization of Fe_3O_4@SiO_2 by APTMS

The silica-coated MNPs (1 g) was treated with triethylamine (75 µL) and (3-aminopropyl) trimethoxysilane 97% (1.2 mL) in toluene (40 mL) in order to introduce amino groups onto the Fe_3O_4@SiO_2 surface. The mixture was treated at 110 °C for 3 h under nitrogen atmosphere and constant stirring. The amino-functionalized nanoparticles (Fe_3O_4@SiO_2-NH_2) were separated from the mixture by applying an external magnet. The Fe_3O_4@SiO_2-NH_2 nanoparticles were washed with ethanol and after that with distilled water. Finally, the functionalized MNPs were dried at room temperature. The chemical procedure is shown at Scheme 1.

Lipase immobilization

20 mg of Fe_3O_4@SiO_2-NH_2 was added to 1 mL HPLC water; the mixture sonicated for 20 min; after that, 60 mg of lipase mixture (TLL:CALB or RML:CALB) at different ratios 0.5:1- 1:1- 1.5:1- 2:1 and 2.5:1 were added to Fe_3O_4@SiO_2-NH_2 in water. Immobilization was started by adding 6 µL of cyclohexyl isocyanide for RML:CALB and 4 µL for TLL:CALB under gentle stirring, followed by incubation at 25 °C for 3–7 h for RML:CALB and 2-3 h for TLL:CALB. Samples of the supernatant were withdrawn and analyzed for determination of the protein concentration by the Bradford's method, the amount of lipase bound to the carrier was determined as the difference between the initial and residual protein concentration [30]. Finally, co-immobilized derivatives were separated by an external magnet and washed by distilled water and stored at 4 °C.

The yield of immobilizations was calculated based on the ratio of the protein attached to the support to the initial amount of the protein (Eq. 1). B_0 is initial and B_1 is residual protein concentration

$$\text{The yields of immobilization (\%)} = \left[B_0 - B_1/B_0\right] \times 100. \quad (1)$$

Enzyme activity assay

The activity of the co-immobilized derivatives was quantified by the release of *p*-nitrophenol during the hydrolysis of *p*-nitrophenyl butyrate (*p*-NPB) in 25 mM sodium phosphate buffer (pH 8.2) at room temperature. Specific activity is given as 1 µmol of *p*-nitrophenol released per minute per mg of the enzyme (IU) under the conditions described as follows. Briefly, 0.01–0.1 mL of the immobilized lipase

suspension or solution (blank or supernatant without further dilution) was added to 2 ml of sodium phosphate buffer (25 mM, pH 8.2) containing 20 µL of *p*-NPB (0.3 mM). The *p*-NPB hydrolysis was then followed spectrophotometrically by measuring the increment in absorbance at 410 nm for 2 min at room temperature.

Characterization of the carrier and co-immobilized biocatalysts

Characterization of the synthesized $Fe_3O_4@SiO_2$ derivatives was carried out using X-ray diffraction analysis (XRD), scanning electron microscopy (SEM), and FT-IR spectroscopy. The size and morphology of magnetic nanoparticles were investigated through scanning electron microscopy with KYKY-EM3200. The images were digitized under the following files: voltage 25.0 kV; probe size, 3.0 nm and magnification, 20,000–80000x. Infrared analysis of the solid samples was collected by FT-IR Bruker in the range of 4000–400 cm^{-1} and the X-ray diffraction measurements were obtained on an STOE-STADV Powder Diffraction System and taken from 1° to 80° (2θ value) using 1.54060 Cu radiation.

Thermal stability of the immobilized preparations

Investigation of thermal stability of the free and co-immobilized lipases (TLL:CALB 1:1 and RML:CALB 1:1) was carried out by incubation of appropriate amount of the free lipases and their co-immobilized derivatives in 400 µL of 25 mM phosphate buffer, pH 7.2 at 35–70 °C (with 5 °C intervals). The samples were incubated for 2 h and their activities were measured using the *p*-NPB assay described above. The residual activity was calculated as the ratio between the remaining activity at a given time and the initial activity of each biocatalyst.

Organic solvent stability

The stability of free lipases and their co-immobilized derivatives (TLL:CALB 1:1 and RML:CALB 1:1) in four organic solvents, including methanol, ethanol, and 1-propanol, was investigated at 25 °C. The appropriate amount of each biocatalyst was added to a 25 mM (pH 7.2) sodium phosphate buffer, containing 10, 20, and 50 vol.% of each solvent. Samples were incubated for 24 h, and their residual activity was calculated as the ratio between the remaining activity and the initial activity of each biocatalyst.

Effect of pH on enzyme activity

To determine the pH activity profile of CALB, RML, TLL, and their co-immobilized derivatives (TLL:CALB 1:1 and RML:CALB 1:1), the activity assays were carried out over a pH range of 5.0–10.5 in 2 ml of 25 mM phosphate buffer at 25 °C. Each set of experiments were performed in triplicate and the average values were calculated.

Biodiesel production

The enzymatic FAME production was carried out according to each design points and the results of FAME yield was used as the response values to optimize the reaction conditions. The reaction was performed in 4 mL screw-capped vials containing 130 mg waste cooking oil and anhydrous methanol, at an oil-to-methanol molar ratio of 1:3. Methanol was added by a three-step procedure and each one molar equivalent of methanol was added at the reaction time of 0, 24 h, and 48 h. The mixtures were incubated for 72 h under constant magnetic agitation of 600 rpm at 35, 40, 45, 50, and 55 °C. At the end of the reaction, an aliquot of the reaction medium was taken, and analyzed by the gas chromatography (GC) method as described below.

GC analysis of fatty acid methyl ester

The oil phase of the reaction mixture was separated by centrifugation at 7000 rpm for 7 min. 20 µL of treated sample was mixed with 1000 µL of 0.8 mg/mL methyl laurate in *n*-hexane. The reaction products were monitored by injecting 0.6 µL of the sample into capillary column gas chromatography (Thermo-Quest-Finnigon) equipped with a flame-ionization detector (FID). Zebron capillary column (30 m × 0.25 mm i.d.; Phenomenex, USA.). Nitrogen as carrier gas at a constant pressure of 0.8 mL/min was used. The injector and FID temperature were set at 150 and 300 °C, respectively. The oven temperature was initially held at 150 °C for 1 min and then increased to 210 °C at 25 °C / min, finally to 240 °C at 10 °C /min and held for 8 min

$$C = \frac{\sum A - A_{IS}}{A_{IS}} \times \frac{C_{IS} \times V_{IS}}{m} \times 100\% , \quad (2)$$

where C = Conversion (FAME yield), $\sum A$ = total peak area; A_{IS} = internal standard (methyl laurate) peak area; C_{IS} = concentration of the internal standard solution in mg/mL; V_{IS} = volume of the internal standard solution used in mL; m = mass of the sample, in mg.

Experimental design

The biodiesel synthesis from waste cooking oil was developed and optimized using response surface methodology (RSM) provided by Design Expert software version 10.0.7 (State Ease Inc, Minneapolis, USA). A 5-level-5 factor central composite design was employed to fit a second-order

Table 1 Immobilization efficiency and specific activity of TLL:CALB co-immobilized on Fe_3O_4@SiO_2

Enzyme ratio	Amount of immobilized enzyme (mg/g support)	Immobilization yield (%)	Immobilization time (h)	Specific activity U/mg
TLL:CALB				
0.5:1	55.2	92	3	30.0
1:1	60.0	100	3	33.7
1.5:1	60.0	100	2	35.3
2:1	60.0	100	3	34.3
2.5:1	60.0	100	3	29.3
RML:CALB				
0.5:1	58.7	97	3	34.1
1:1	60.0	100	5	32.8
1.5:1	56.7	94	7	32.4
2:1	58.2	97	6	33.8
2.5:1	60.0	100	3	21.2

Fe_3O_4@SiO_2-NH_2-TLL 16.15 (U/mg), Fe_3O_4@SiO_2-NH_2-CALB 16.24 (U/mg), Fe_3O_4@SiO_2-NH_2-RML, 16.08 (U/mg), free TLL 27.5 (U/mg), free CALB 49.5 (U/mg), and free RML 52.98 (U/mg)

response surface model which requires 45 experiments, including 32 factorial points, 10 axial points, and 3 replicates at the center points. The center points were repeated 3 times to determine the experimental error (pure error) and the reproducibility of the data. The parameters [21, 25] for designing reactions were based on our previous reports about using multi-component reactions for enzyme immobilization.

Five identified independent variables were A: reaction temperature (35–55 °C), B: enzyme-to-oil ratio (5–25 wt.%), C: water for TLL:CALB (0–40 wt.%)/ water adsorbent (blue silica gel) for RML:CALB (20–60 wt.%), D: *t*-butanol ratio to oil (10–50 wt.%), and E: TLL:CALB or RML:CALB (0.5:1—2.5:1); each independent variables level were chosen based on our previous investigations. The independent variables are coded to two levels to be precise low (-1) and high (+1). The axial points are coded as -2 (-α) and +2 (+α). In this research, the α value was fixed at 2 which is the distance of the axial point from center and makes the design rotatable.

Reusability

The enzyme reuse was evaluated in the transesterification reaction of waste cooking oil with methanol (oil:methanol ratio 1:3), co-immobilized TLL:CALB (1:1) or RML:CALB (1:1), enzyme-to-oil ratio (10 wt.%), and water for TLL:CALB (20 wt.%)/water adsorbent (blue silica gel) for RML:CALB (20 wt.%). After methanolysis reactions, immobilized lipases were separated by centrifugation (4000 rpm, 5 min) and washed with *n*-hexane three times, and then, the lipase derivatives were dried in a desiccator for 24 h. This procedure was repeated up to five cycles in the same condition as described above. The ester yield of the first reaction was set as 100% and the ester yield in the subsequent reactions was calculated accordingly.

Results and discussion

Immobilization

The amount of co-immobilized lipases, their specific activity, and immobilization time are shown in Table 1. As can be seen in Table 1 by increasing CALB:RML and CALB:TLL ratio from 1:1 to 2.5:1, the amount of immobilized enzyme on the support is almost the same for all ratios. The specific activity of free CALB and RML (49.5 and 52.9 U/mg, respectively) decreased to 29–35 and 21–34 U/mg after immobilization for TLL:CALB and RML:CALB, respectively, which is common phenomenon after immobilization due to secondary structural changes. For all ratios in both co-immobilized system, there is no remarkable increase or decrease in specific activity from 0.5:1—2:1 but by further increase of CALB to 2.5:1 in both preparations a decrease in specific activity was observed. Covalent co-immobilization of RML:CALB and TLL:CALB on Fe_3O_4@SiO_2-NH_2 was performed via an isocyanide-based multi-component reaction approach. In this way, amino-functionalized Fe_3O_4@SiO_2 supplies amine group to react with an intermediate already formed by the reaction between cyclohexyl isocyanide and carboxylic acid groups of lipase [31, 32].

Co-immobilization of RML:CALB (4–15 mg/g) on epoxy functionalized silica gel in our previous report was carried out in 6 h [21], but in this report via isocyanide-based multi-component reaction, TLL:CALB and RML:CALB (60 mg/g) were immobilized on amino-functionalized Fe_3O_4@SiO_2 in 2 and 3 h, respectively, which is showing

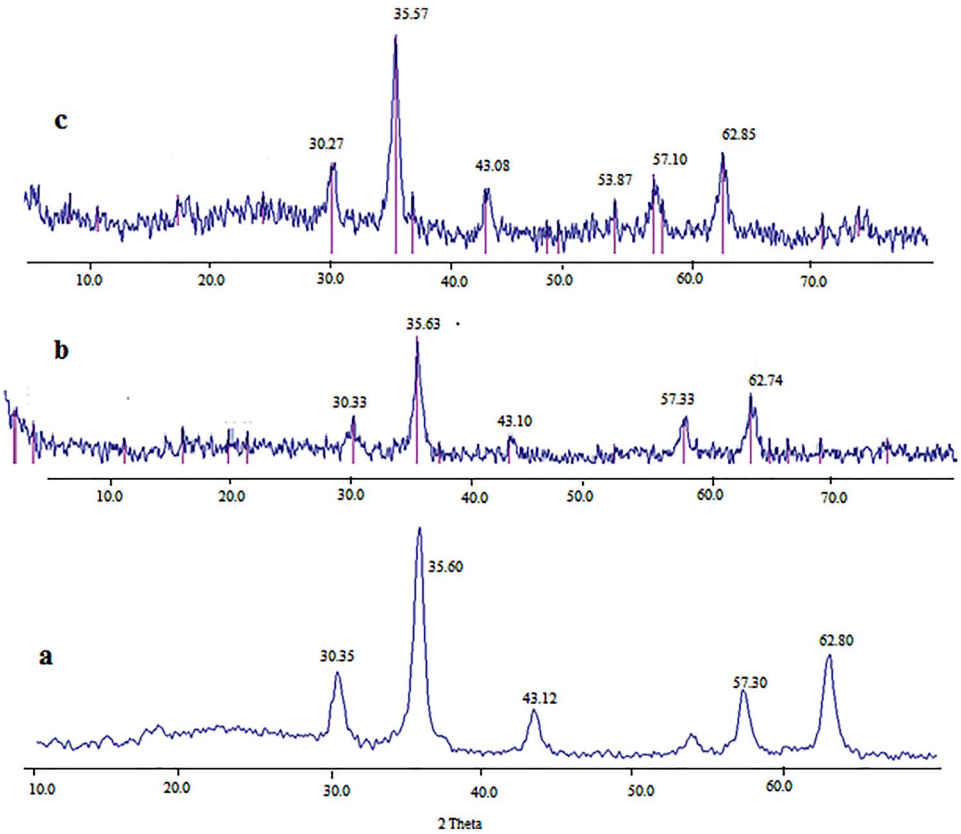

Fig. 1 XRD patterns; **a** Fe_3O_4@SiO_2 core–shell magnetic nanoparticles (Fe3O4@SiO2s), **b** amino-functionalized magnetic nanoparticles (Fe_3O_4@SiO_2-NH_2), and **c** Fe_3O_4@SiO_2-NH_2-TLL-CALB

dramatically decrease in immobilization time and increase in immobilization yield. In another study, Mohammadi et *al*. in 2016 reported rapid immobilization of enzyme (30 min) via a three-component immobilization reaction that use epoxide groups from the support, isocyanide as an additive and carboxylic acids from enzyme. The results showed in the absence of isocyanide 95% immobilization yield was achieved after 24 h of incubation. The loading of the supports was also dramatically improved in this method with persevering the specific activity [33].

An enzyme loading of 55.2–60 mg/g support was achieved for TLL:CALB, corresponding to 91–100% enzyme loading. For RML:CALB, the enzyme loading was 56.7–60 mg/g support with 94–100% enzyme loading efficiency. More surprisingly, the results for RML:CALB and TLL:CALB showed co-immobilization causes to increase in enzyme specific activity compared to the individually immobilized enzymes Fe_3O_4@SiO_2-NH_2-TLL, Fe_3O_4@SiO_2-NH_2-RML, and Fe_3O_4@SiO_2-NH_2-CALB.

Characterization

XRD pattern

To identify the crystalline structure of Fe_3O_4 MNPs, their X-Ray Diffraction (XRD) pattern was investigated (Fig. 1 a–c). As can be seen, the existence of a peak around the angle (2θ) equal to 35.63° confirms the formation of spinal ferrites [34]. All the strong peaks observed at (2θ = 30.27°, 35.57°, 43.08°, 53.87°, 57.10°, and 62.85°) are indexed to the highly crystalline cubic spinel structure of Fe_3O_4 nanoparticles (compared with the JCPDS 01–088-0315 data file) [35]. The same sets of characteristic peaks for all Fe_3O_4@SiO_2, Fe_3O_4@SiO_2-NH_2, and Fe_3O_4@SiO_2-NH_2-TLL-CALB indicate the stability of the crystalline phase of Fe_3O_4 nanoparticles during silica coating, surface amine functionalization, and enzyme immobilization.

Infrared spectroscopy analysis IR

FT-IR spectroscopy was used to confirm the functionalization of the supports. In Fig. 2 (a–f), the spectra of (a) Fe_3O_4@SiO_2, (b) amino-functionalized magnetic nanoparticles (Fe_3O_4@SiO_2-NH_2), (c) Fe_3O_4@SiO_2-NH_2-TLL-CALB and free TLL, RML, and CALB (e, d, f) are presented. In Fig. 2a, the peaks at 809.67 and 1096.44 cm^{-1} refer to the symmetric stretching of Si–OH and Si–O-Si, respectively; also, the broad band about 3400 cm^{-1} could be attributed to the O–H-stretching frequency of silanol group which can be seen only for the silica-coated nanoparticles. Absorption bands due to the (Fe–O) are observed in the 450–550 cm^{-1}. In the IR spectra of pure lipases Fig. 2 (e–f),

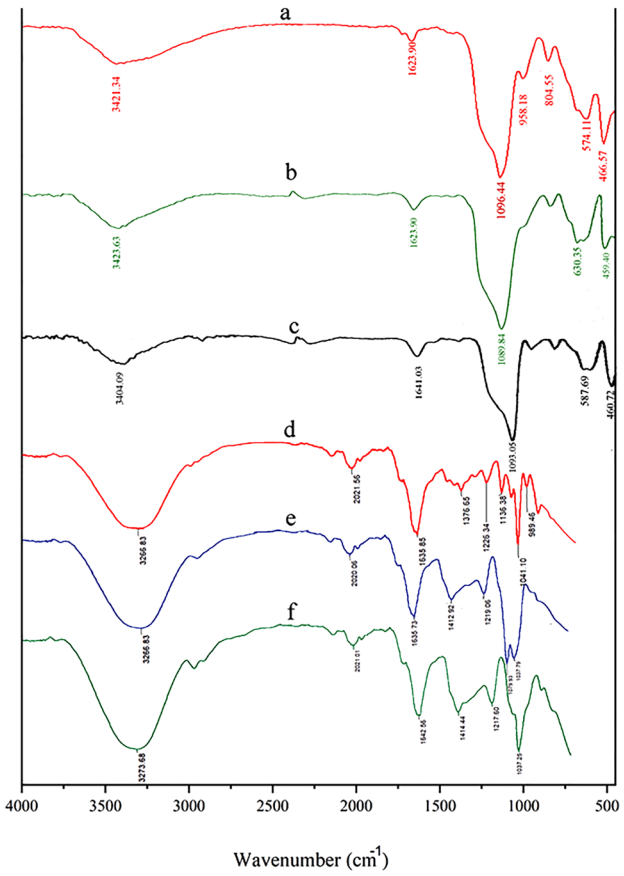

Fig. 2 FT-IR spectra of: **a** Fe_3O_4@SiO_2 core–shell magnetic nanoparticles (Fe_3O_4@SiO_2), **b** amino-functionalized magnetic nanoparticles (Fe_3O_4@SiO_2-NH_2), **c** Fe_3O_4@SiO_2-NH_2-TLL-CALB, **d** free TLL, **e** free RML, and **f** free CALB

many characteristic bands of the amino acids such as the C=O bond of the amino acid in the region 1630–1640 cm^{-1}, and OH-stretching band at 3200 cm^{-1} are observed.

Scanning electron microscopy (SEM)

Surface morphology of synthesized Fe_3O_4@SiO_2, Fe_3O_4@SiO_2-NH_2 and co-immobilized derivatives (Fe_3O_4@SiO_2-NH_2-TLL-CALB) were observed through SEM (Fig. 3a–c). The final product of the synthesis consists of several bunches of spherical shaped in several micron sizes. SEM analysis was utilized to display the spherical morphology of the support remains unchanged through the functionalization and immobilization process. It can be concluded that the modification still preserving the textural properties of the parent support such as many previous reports [36, 37].

Thermal stability of the immobilized enzyme

Figure 4 shows the time course of residual activity of crude CALB, TLL, RML, and their co-immobilized derivatives at different temperatures (35–70 °C). The thermal stability of co-immobilized derivatives at all temperatures decreased gradually [38]. At the lowest temperature (35 °C), all the free and co-immobilized enzymes preserved their activities. At 45 °C, free RML and CALB showed only 70% residual activity at 2 h, whereas Fe_3O_4@SiO_2-NH_2-RML-CALB completely retained its activity. Increasing the temperature to 55 °C clearly unraveled the difference in the stability of biocatalyst. While RML:CALB and TLL:CALB preserved completely their activity, free TLL, RML, and CALB

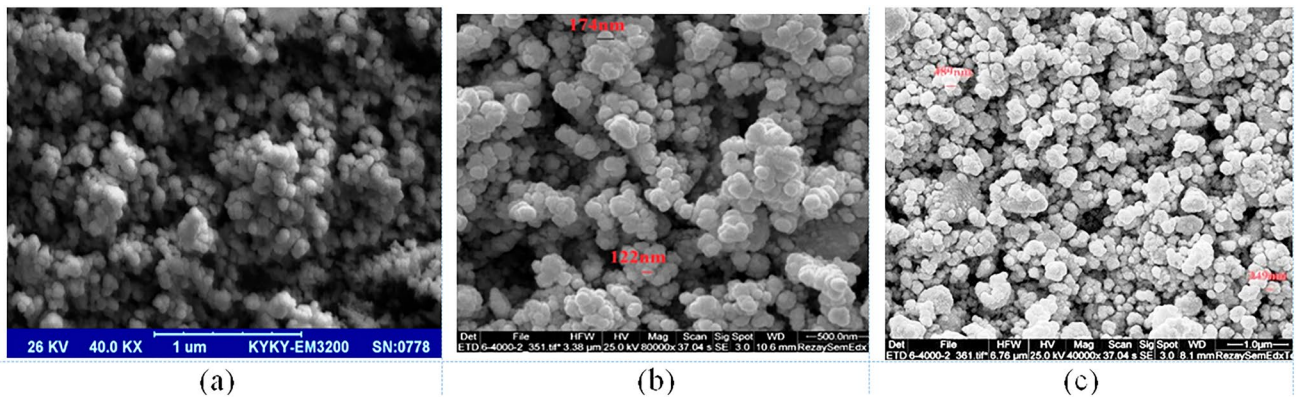

Fig. 3 SEM images of synthesized: **a** Fe_3O_4@SiO_2 core–shell magnetic nanoparticles (Fe_3O_4@SiO_2), **b** amino-functionalized magnetic nanoparticles (Fe_3O_4@SiO_2-NH_2), and **c** Fe_3O_4@SiO_2-NH_2-TLL-CALB

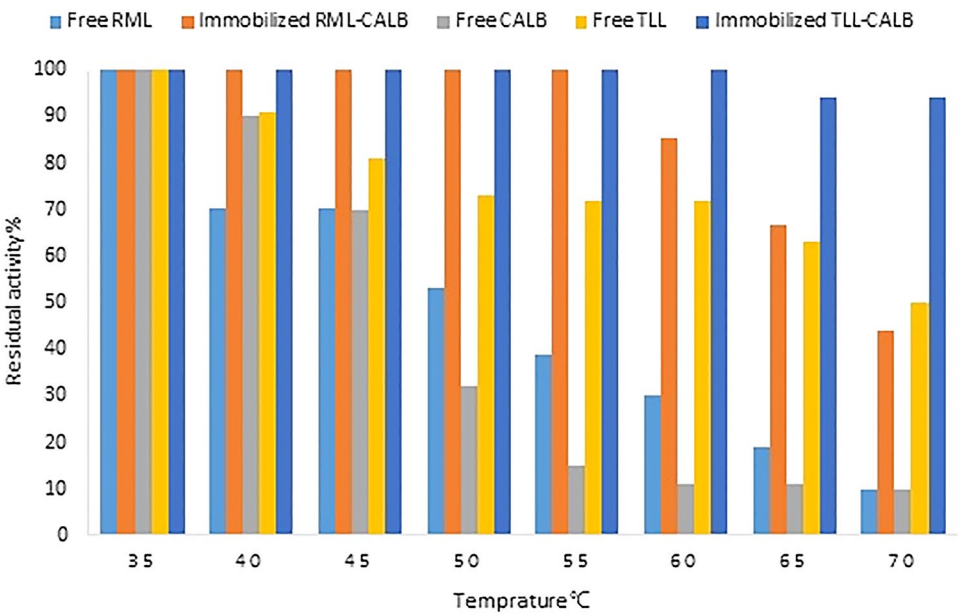

Fig. 4 Thermal stability of: Fe_3O_4@SiO_2-NH_2-TLL-CALB, Fe_3O_4@SiO_2-NH_2-RML-CALB, free TLL, RML, and CALB in 10 mM sodium phosphate buffer pH 7.2 and incubation at different temperatures

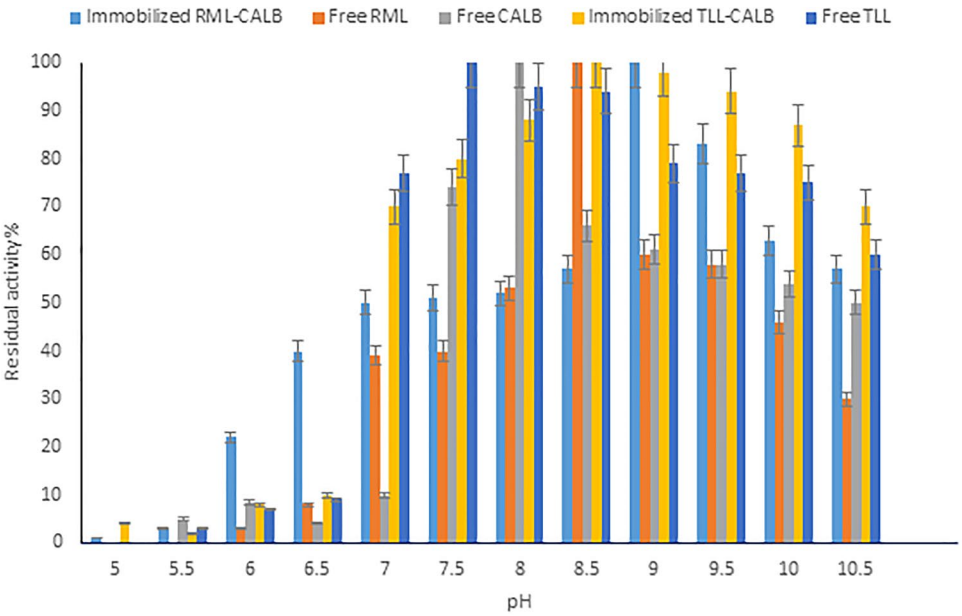

Fig. 5 Stability of Fe_3O_4@SiO_2-NH_2-TLL-CALB, Fe_3O_4@SiO_2-NH_2-RML-CALB, free CALB, free TLL, and free RML in different pH values at 25 °C

activity decreased to 72, 39, and 15% of their initial activity, respectively. At 70 °C, Fe_3O_4@SiO_2-NH_2-RML-CALB deactivated to less than 50% residual activity, while Fe_3O_4@SiO_2-NH_2-TLL-CALB kept 90% of initial activity. At this temperature, the tertiary structure of the enzyme is altered drastically leading to protein unfolding [39]. Apparently, co-immobilized lipases on Fe_3O_4@SiO_2 showed better thermal stabilities than those free forms, since covalent attachment provides strong binding interaction between lipase and support that reduces the occurrence of drastic conformational changes and enhances glycoprotein's structural rigidity.

Effect of pH on immobilized enzyme activity

The effect of pH on the activity of free and co-immobilized lipases on Fe_3O_4@SiO_2 was investigated at different pH values from 5.0 to 10.5 and the results are presented in Fig. 5. The free and co-immobilized lipase both exhibited maximum activity at pH 7.0–9.0. It can be concluded that both lower and higher pH values are unfavourable for enzymatic activity of the lipase. This could be due to the changes in the enzyme structure and ionic states of the active site residues; though, the co-immobilized enzymes showed higher stability at alkaline conditions (pH 9.0). Other ratios of co-immobilized derivatives presented similar results.

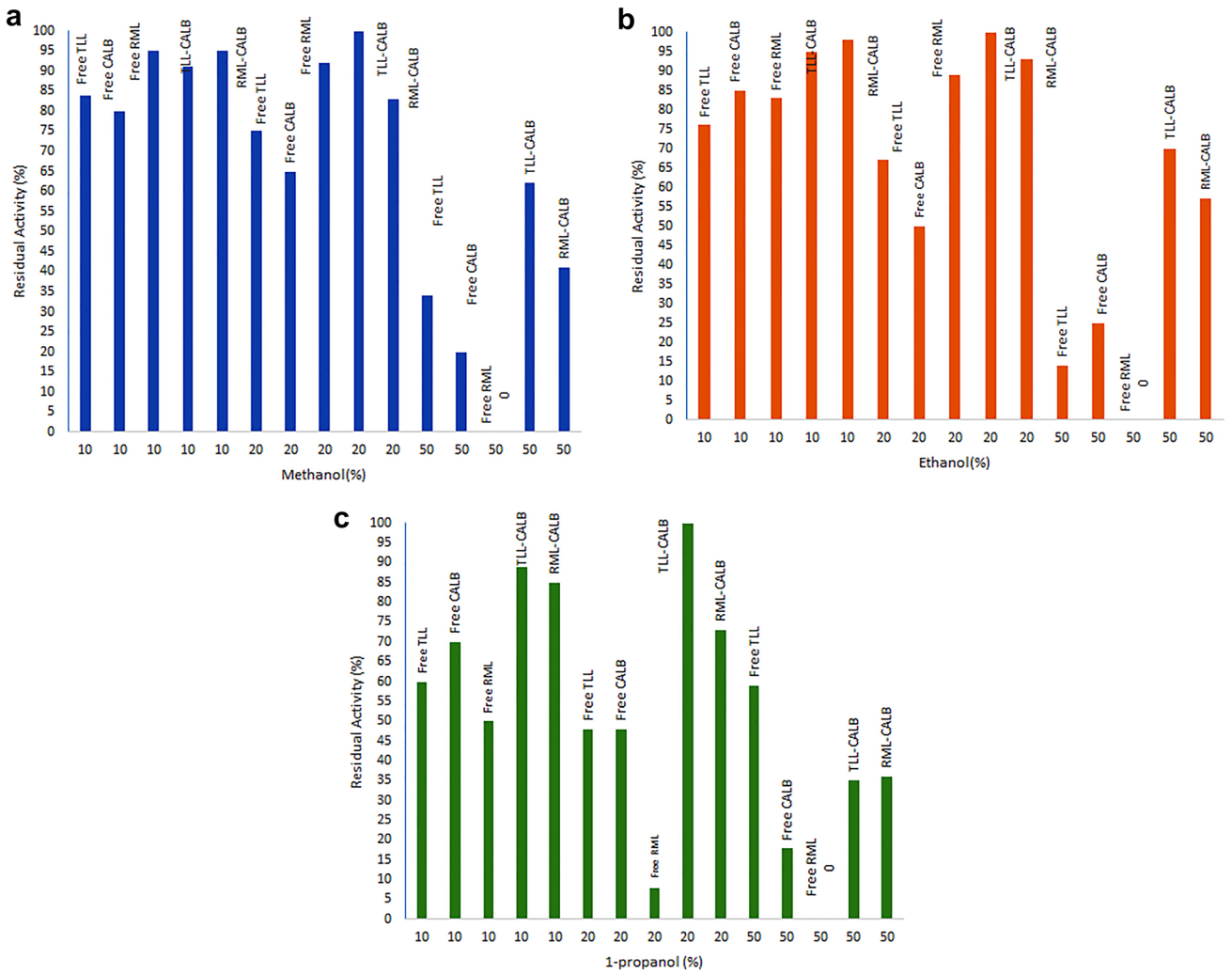

Fig. 6 Stability of co-immobilized derivatives Fe_3O_4@SiO_2-NH_2-TLL-CALB and Fe_3O_4@SiO_2-NH_2- RML-CALB in various co-solvent: **a** methanol, **b** ethanol, and **c** 1-propanol

Organic solvent stability

In most of the enzymatic reactions, the use of organic solvents is inevitable. Enzymes could maintain high catalytic activity in organic solvents that are rather hydrophobic, whereas in those organic solvents with log $p < 2$, the enzyme would lose its activity very rapidly. This is because a few amounts of water molecules are required for enzymatic function, and usually, polar organic solvents tend to strip this essential water and decrease the catalytic activity of lipase [40]. The deleterious effect of organic solvents on lipase enzymes can be eliminated by using immobilized enzyme preparations. The stability of the covalently immobilized preparations compared to the free lipases in the presence of methanol, ethanol, and 1-propanol is shown in Fig. 6a–c. Both co-immobilized derivatives revealed improved stability in the presence of the four organic co-solvents compared to the soluble enzymes.

Fe_3O_4@SiO_2-NH_2-TLL-CALB and Fe_3O_4@SiO_2-NH_2-RML-CALB retained most of their activity in presence of 10 and 20 vol.% of all solvents after 24 h of incubation, while the free enzymes lost 10–50% of their activity at the same condition.

Optimization of biodiesel production

Design expert software 10.0.7 program was used to calculate the effect of each factor and its interactions. Central composite design (CCD) was carried out to optimize the transesterification of waste cooking oil using co-immobilized lipases. The waste cooking oil methyl ester yield was from 33 to 99% for RML-CALB and 27–81% for TLL-CALB system.

Table 2 Sequential model sum of squares (RML:CALB)

Source	Sum of squares	df	Mean square	*F* value	Prob > F	
Mean vs total	2.476E + 005	1	2.476E + 005			Suggested
Linear vs mean	2570.90	5	514.18	1.71	0.1560	
2FI vs Linear	4564.28	10	456.43	1.84	0.0971	
Quadratic vs 2FI	2365.78	5	473.16	2.36	0.0711	Suggested
Cubic vs quadratic	3338.97	15	222.60	1.35	0.3299	Aliased
Residual	1479.77	9	164.42			
Total	2.619E + 005	45	5820.06			

Among the models that fitted to the response, the quadratic model was selected as the best model due to its highest order polynomial with significance of additional terms and model was not aliased. This quadratic model was suggested by the RSM software as shown in Table 2 for RML:CALB and Table 3 for TLL:CALB. For waste cooking oil along with the dependent variable fit FAME conversion (R_1) was analyzed using RSM. As a result, the second-order polynomial Eq. 3 (for RML:CALB) and Eq. 4 (for TLL:CALB) in the form of model could be obtained

$$\begin{aligned} R_1 = {} & +84.90 + 6.63 * A + 2.19 * D - 3.28 * E \\ & -2.50 * AB - 5.50 * AD + 6.99 * AE - 5.01 * BC \\ & +4.47 * BD - 3.04 * BE - 4.55 * B^2 - 7.51 * C^2 \end{aligned} \quad (3)$$

$$\begin{aligned} R_1 = {} & +46.52 - 1.74 * A - 0.37 * B - 0.72 * C \\ & -0.54 * D + 0.83 * E - 0.56 * AC + 3.76 * AD \\ & -5.05 * AE\ 0.31 * BC + 4.53 * BD + 0.80 * BE \\ & +0.43 * CD - 1.36 * CE - 4.60 * DE. \end{aligned} \quad (4)$$

Positive sign in front of the terms indicates synergistic effect in growth of FAME yield, while negative sign points out antagonistic effect. The results at each point based on the central composite design (CCD) and their corresponding values are presented in Table 4 (RML:CALB) and Table 5 (TLL:CALB). The result of statical analysis of variance (ANOVA) which was carried out to define the significance (by *F* Test) and fitness of the quadratic model as well as the effect of significant individual terms and their interaction on the selected responses are presented in Table 1S for RML:CALB and Table 2S for TLL:CALB. The F value of 4.78 (RML:CALB) and 7.67 (TLL:CALB) with p value < 0.0002 (RML:CALB) and < 0.0001 (TLL:CALB) implies that the model is significant at 95% confidence level. The p value (probability of error value) is used as a tool to check the significance of each regression coefficient, which also indicate the interaction effect of each cross product; the smaller the p value, the bigger the significance of the corresponding coefficient is. Among all factors for both systems (TLL:CALB and RML:CALB), the temperature was significant (p value < 0.05), but since significant interaction of other factors with temperature, the other factors are also presents in proposed models.

The R^2 value of 0.78 for TLL:CALB, 0.61 for RML:CALB and adjusted R^2 0.68 for TLL:CALB, 0.49 for RML:CALB shows that the model could be used predicting the response. The predicted R-squared (a measure of the amount of variation in new data explained by the model) and the adjusted R-squared (a measure of the amount of variation around the mean explained by the model) should be within 0.20 of each other. Otherwise, there may be a problem with either the data or the model.

In the case of model terms, the p values less than 0.05 indicated that the particular model terms were statistically significant. A low value of coefficient of the variation (CV: 17.44% for RML:CALB and 11.14% for TLL:CALB) indicated high degree of precision and a good deal of reliability of the experimental values. The lack of fit test with p value of 0.1259 (RML:CALB) and 0.4866 (TLL:CALB), which is not significant (p value > 0.05 is not significant),

Table 3 Sequential model sum of squares (TLL:CALB)

Source	Sum of squares	df	Mean square	*F* value	Prob > F	
Mean vs total	97,386.27	1	97,386.27			
Linear vs mean	186.58	5	37.32	0.42	0.8354	
2FI vs linear	2699.97	10	270.00	9.71	< 0.0001	Suggested
Quadratic vs 2FI	34.57	5	6.91	0.22	0.9527	
Cubic vs quadratic	457.59	15	30.51	0.87	0.6069	Aliased
Residual	313.90	9	34.88			
Total	1.011E + 005	45	2246.20			

Table 4 Experimental design for five-level five-factor surface response design on transesterification and esterification of waste cooking oil using co-immobilized RML:CALB

Run	Type	A: reaction temperature (°C)	B: enzyme (wt.%)	C: water adsorbent (wt.%)	D: *t*-butanol ratio (wt.%)	E:RML:CALB ratio	FAME yield (%)	Predicted fame yield (%)
1	Fact	50	20	30	40	1.0	95.9	85.4
2	Fact	50	10	30	20	1.0	99.0	77.0
3	Axial	45	15	60	30	1.5	68.1	52.9
4	Fact	50	10	50	40	2.0	84.1	83.0
5	Fact	50	20	30	40	2.0	75.1	86.7
6	Fact	40	20	30	40	1.0	91.6	102.1
7	Axial	45	15	40	50	1.5	86.9	89.3
8	Fact	40	20	30	20	2.0	50.5	51.2
9	Axial	45	15	40	10	1.5	79.5	80.5
10	Axial	55	15	40	30	1.5	77.4	98.1
11	Fact	50	10	50	20	1.0	88.8	85.1
12	Fact	50	20	50	20	1.0	52.8	71.1
13	Fact	50	10	30	20	2.0	86.1	90.5
14	Fact	40	10	30	20	1.0	59.9	61.7
15	Center	45	15	40	30	1.5	94.6	84.9
16	Fact	50	10	30	40	1.0	49.7	61.4
17	Fact	40	10	30	40	1.0	64.6	68.1
18	Fact	40	20	30	20	1.0	85.3	77.8
19	Fact	40	10	50	20	1.0	65.7	69.8
20	Axial	45	25	40	30	1.5	83.0	70.6
21	Fact	50	20	50	20	2.0	89.5	72.5
22	Fact	40	20	30	40	2.0	77.8	75.5
23	Axial	45	15	20	30	1.5	49.6	56.8
24	Fact	40	20	50	20	2.0	33.4	39.2
25	Fact	50	20	30	20	2.0	97.1	84.4
26	Axial	45	5	40	30	1.5	58.4	62.8
27	Axial	35	15	40	30	1.5	82.4	71.6
28	Fact	50	10	30	40	2.0	97.4	74.9
29	Fact	50	10	50	40	1.0	62.5	69.5
30	Axial	45	15	40	30	2.5	76.2	78.3
31	Fact	40	20	50	40	1.0	90.2	90.2
32	Fact	40	10	50	20	2.0	59.1	55.3
33	Fact	40	10	50	40	2.0	63.6	61.8
34	Axial	45	15	40	30	0.5	94.7	91.5
35	Fact	40	20	50	20	1.0	51.8	65.9
36	Center	45	15	40	30	1.5	89.3	84.9
37	Fact	50	20	50	40	1.0	94.7	73.5
38	Fact	40	10	50	40	1.0	76.2	76.2
39	Fact	40	20	50	40	2.0	52.6	63.5
40	Fact	40	10	30	20	2.0	37.8	47.2
41	Fact	50	10	50	20	2.0	88.3	98.6
42	Center	45	15	40	30	1.5	99.0	77.0
43	Fact	50	20	30	20	1.0	67.5	83.1
44	Fact	40	10	30	40	2.0	51.5	53.7
45	Fact	50	20	50	40	2.0	58.1	74.8

Table 5 Experimental design for five-level five-factor surface response design on transesterification and esterification of waste cooking oil using co-immobilized TLL:CALB

Run	Type	A: reaction temperature (°C)	B: enzyme (wt %)	C: water (wt %)	D: *t*-butanol ratio (wt %)	E: TLL:CALB ratio	FAME yield (%)	Predicted FAME yield (%)
1	Fact	40	10	30	20	2.0	63.6	65.5
2	Axial	45	25	20	30	1.5	47.6	45.8
3	Axial	45	5	20	30	1.5	43.5	47.3
4	Fact	40	10	10	20	2.0	81.0	68.8
5	Fact	50	20	10	40	2.0	50.9	46.6
6	Axial	45	15	20	10	1.5	43.1	47.6
7	Center	45	15	20	30	1.5	49.8	46.5
8	Fact	50	10	10	20	2.0	42.5	48.8
9	Fact	40	20	30	20	1.0	33.7	36.8
10	Axial	45	15	0.0	30	1.5	41.6	47.9
11	Fact	50	20	10	40	1.0	55.7	60.0
12	Fact	50	10	30	40	2.0	27.9	32.3
13	Fact	50	10	30	20	2.0	45.1	43.3
14	Fact	50	10	10	20	1.0	47.6	46.9
15	Axial	55	15	20	30	1.5	43.2	43.0
16	Axial	45	15	40	30	1.5	43.5	45.1
17	Fact	40	20	10	20	1.0	36.0	35.9
18	Fact	40	20	10	40	2.0	48.1	51.6
19	Axial	45	15	20	30	2.5	42.9	48.2
20	Fact	40	20	10	40	1.0	53.2	44.7
21	Axial	35	15	20	30	1.5	47.7	50.0
22	Fact	40	10	30	20	1.0	46.5	48.8
23	Fact	50	20	30	20	2.0	37.6	34.4
24	Fact	40	10	10	40	2.0	37.3	41.1
25	Fact	50	20	30	20	1.0	36.1	34.8
26	Axial	45	15	20	50	1.5	40.9	45.4
27	Fact	50	20	30	40	2.0	43.2	41.6
28	Fact	50	20	10	20	1.0	39.8	36.1
29	Fact	50	20	30	40	1.0	56.2	60.4
30	Center	45	15	20	30	1.5	48.2	46.5
31	Fact	40	10	10	40	1.0	32.6	37.4
32	Fact	40	10	30	40	2.0	43.1	39.5
33	Center	45	15	20	30	1.5	41.7	46.5
34	Fact	40	20	30	40	1.0	48.6	47.4
35	Fact	40	20	30	20	2.0	58.0	56.7
36	Fact	40	10	10	20	1.0	47.9	46.7
37	Fact	50	20	10	20	2.0	38.3	41.2
38	Axial	45	15	20	30	0.5	42.3	44.9
39	Fact	50	10	10	40	2.0	46.0	36.1
40	Fact	40	20	30	40	2.0	49.7	48.8
41	Fact	50	10	10	40	1.0	55.8	52.6
42	Fact	40	20	10	20	2.0	62.1	61.2
43	Fact	50	10	30	20	1.0	51.3	46.8
44	Fact	40	10	30	40	1.0	47.6	41.3
45	Fact	50	10	30	40	1.0	54.1	54.3

disclosed that the model satisfactorily fitted to experimental data. Insignificant lack of fit is most wanted as significant lack of fit indicates that there might be contribution in the regressor–response relationship that is not accounted for by the model. This analysis was examined using the normal probability of the residuals. The normal plot probability plot of the residuals indicates that the errors are distributed normally in a straight line and insignificant. On the other hand, the model does not show any violation of the independence or constant variance assumption.

Regarding the of yield of biodiesel production, the maximum yield for RML:CALB and TLL:CALB in this study was 99 and 80%, respectively.

Also there are also other reports which state that RML (96.3%) had better efficiency than TLL (72.9%) in synthesis of biodiesel from sunflower oil [41], they observed methanolysis progressed faster at the beginning with TLL; however, the reaction yield was lower compared to that found with lipases from RML.

Toro et al. reported Combi-lipases (CL) systems based on mixtures of different lipases immobilized on different supports. The increased CL efficiency was attributed to the complementary selectivity of different lipases. In their report, the role of the immobilization support in CL or in co-immobilized systems was remarkable, since individually immobilized TLL on commercially available supports Purolite®, Lewatit® gave rise to 68.1 and 92.5% fatty acid ethyl esters, respectively [42].

Tiosso and co-workers reported commercially available immobilized TLL (Lipozyme TL-IM) displayed an unsatisfactory performance in the transesterification reaction of different alkyl-chain triglycerides with ethanol (73% the efficiency of biodiesel production) [43].

Parameter study

Fe_3O_4@SiO_2-NH_2-RML-CALB

The optimum combinations for the reaction in RML-CALB co-immobilized system were enzyme-to-oil (20 wt.%), RML:CALB ratio (1:1), *t*-butanol (20 wt.%), temperature (50 °C), and water adsorbent (30 wt.%). This resulted in an FAME yield of 99%.

Acyl migration as a rate-determining step can decrease the efficiency of transesterification reactions. Several factors can promote this non-enzymatic phenomenon, such as increase in temperature [44], low amount of water [45], and the amount of biocatalyst; it has been found that increasing the amount of biocatalyst leads to an increase in efficiency by enhancing acyl migration [46] and consequently higher yields. Also, it can be seen from our results that enzyme-to-oil (20 wt.%) resulted in 99% FAME yield.

As shown in Tables 4 and 5, increasing the amount of catalyst from 5 to 20 wt% increases the efficiency significantly, regarding this fact that the optimal value of catalyst in system is below 20 wt%, the amount of biocatalyst for biodiesel production, which is determined based on the amount of starting material, has various values and varies from 1 to 60% for different immobilized enzymes [47–54]. In previous reports, it has been stated that the increase in catalyst is associated with a decrease in efficiency, and this decrease is due to the increase in the viscosity of the reaction medium and, as a result, enhanced diffusional resistance in heterogeneous biocatalyst [55]. However, in this study, fortunately, increasing the catalyst up to 20% does not cause a disturbance in increasing efficiency, and this is one of the advantages of this study.

Figure 7a shows the 3D plot for an interaction effect between the amount of biocatalyst (B) and reaction temperature (A) toward biodiesel yield. The 3D response surface revealed that increment of reaction temperature from low level (40 °C) to the high level (50 °C) leads to the increase in FAME content at low level of biocatalyst content (10% wt.%) and although the increase of enzyme ratio improved the biodiesel yield at low level of temperature. Alcohols such as *t*-butyl alcohol are good co-solvent for enzyme-catalyzed production of biodiesel; this is because this alcohol could significantly improve the solubility of both methanol and glycerol in the reaction mixture [56]; in Fig. 7b, it can be seen that lower amount of *t*-butanol (20 wt.%) gave rise to higher FAME yield than the higher amount (40 wt.%). Higher conversion in lower amount of *t*-butanol might be due to the dilution effect of solvent in a higher *t*-butanol percentage. Fig 7c reveals the interaction of reaction temperature (A) and the ratio of RML: CALB (E). As can be seen in Fig. 7c in a high level of temperature, a higher ratio of RML:CALB resulted in higher FAME yield. Facilitating acyl migration, which allows biodiesel conversion to reach high levels, is the advantages of co-immobilization of enzymes. The interaction between the amount of enzyme:oil ratio and water-absorbent:oil ratio is shown in Fig. 7d. Water could result in aggregation of the enzyme in hydrophobic media, thus eliminating its catalytic activity, while also having a negative effect on the stability of the enzymes [57]. In the reaction catalyzed by Fe_3O_4@SiO_2-NH_2-RML-CALB, however, at a higher level of the enzyme, the biodiesel yield increased slightly by rising blue silica gel quantity up to 40 wt.%, whereas a further increase in the amount of adsorbent resulted in lower biodiesel production. This could be because of mass transfer problems and negative effect on mixing or the adsorption of methanol onto blue silica gel and lower methanol concentration in the reaction medium.

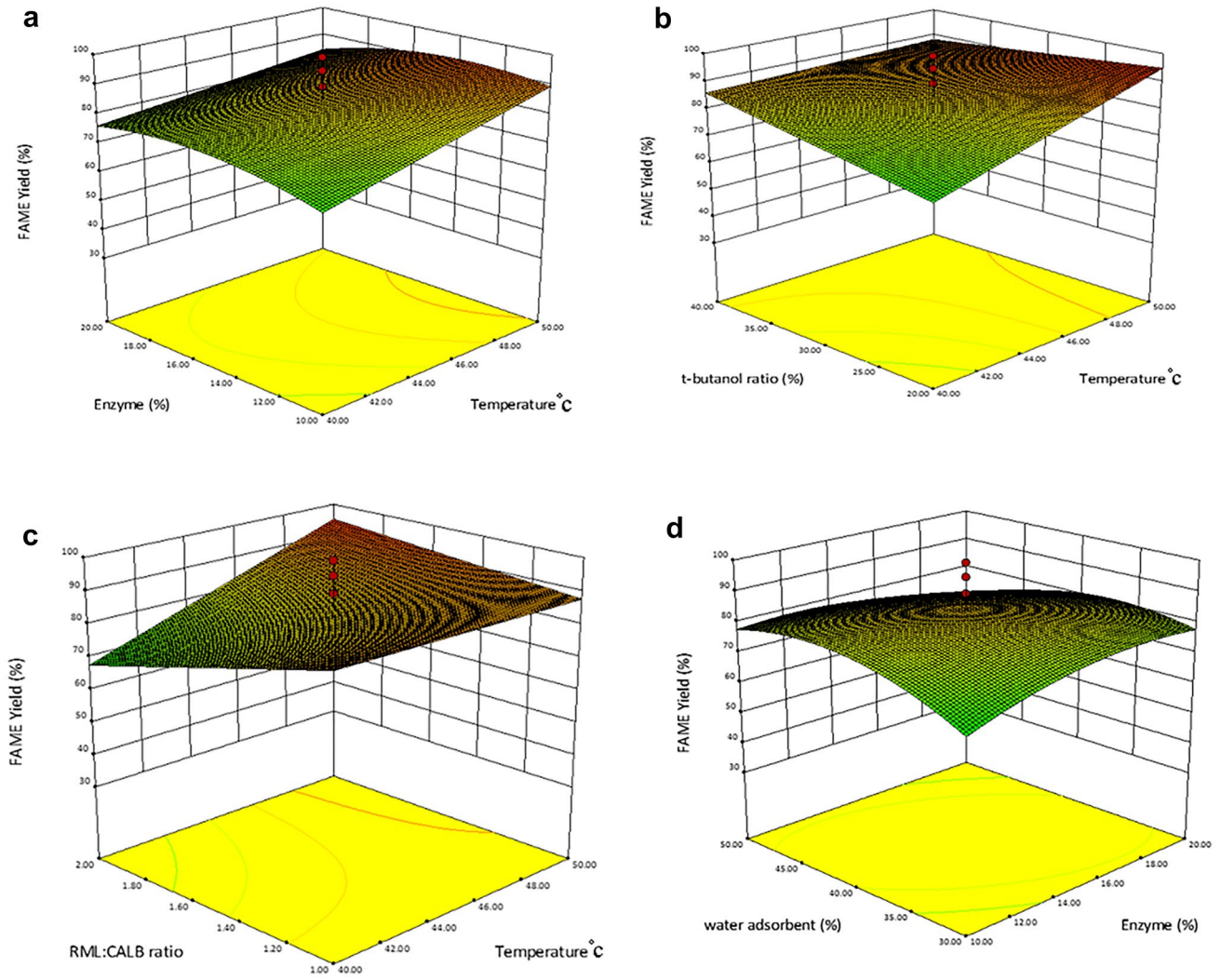

Fig. 7 Response surface plot and contour plot of FAME conversion: **a** enzyme-to-oil ratio vs. temperature (°C), **b** *t*-butanol vs. temperature (°C), **c** RML: CALB ratio vs. temperature (°C), and **d** water-absorbent to oil ratio vs. enzyme-to-oil ratio

Fe_3O_4@SiO_2-NH_2-TLL-CALB

The optimum combinations for the reaction in TLL-CALB co-immobilized system were enzyme percent (10 wt.%) TLL:CALB ratio (2:1), *t*-butanol (20 wt.%), temperature (40 °C), water (10 wt.%). This resulted in a FAME yield of 81%.

Figure 8a illustrates the interaction effect between reaction temperature and *t*-butanol content. Typically, solvents are used to raise the conversion of transesterification reactions. *t*-Butanol has been reported as a suitable solvent for immobilized lipase-mediated conversion of oil to biodiesel [56, 58]. As a result of the steric hindrance of this alcohol, they are not substrates for lipases. Fe_3O_4@SiO_2-NH_2-TLL-CALB catalyzed reactions performed by 20–30 wt.% of *t*-butanol resulted in increasing conversion but further increasing in *t*-butanol concentration gave a lower amount of biodiesel. Figure 8b depicts the interaction between reaction temperature (A) and the ratio of TLL:CALB (E) as can be seen in the low level of temperature, the higher ratio of TLL:CALB improved FAME production. TLL lipase is a 1,3-specific lipase and cannot hydrolyze fatty acids on the second position of 1,2-diglyceride; however, it can move a fatty acid from this position to the third position (acyl migration) which allows biodiesel conversion to reach high rates [59]. Fig. 8c presents the interaction effect of co-solvent and enzyme-to-oil ratio, at a higher level of the enzyme increasing the amount of co-solvent resulted in increasing the FAME yield. It can be seen the co-solvent can decrease the destructive effect of methanol on biocatalyst deactivation. Moreover, FAME production in presence of *t*-butanol also reduces the inhibitory effect of glycerol. Glycerol as a by-product in the transesterification process makes a layer over the surface of the enzyme molecules or the support used

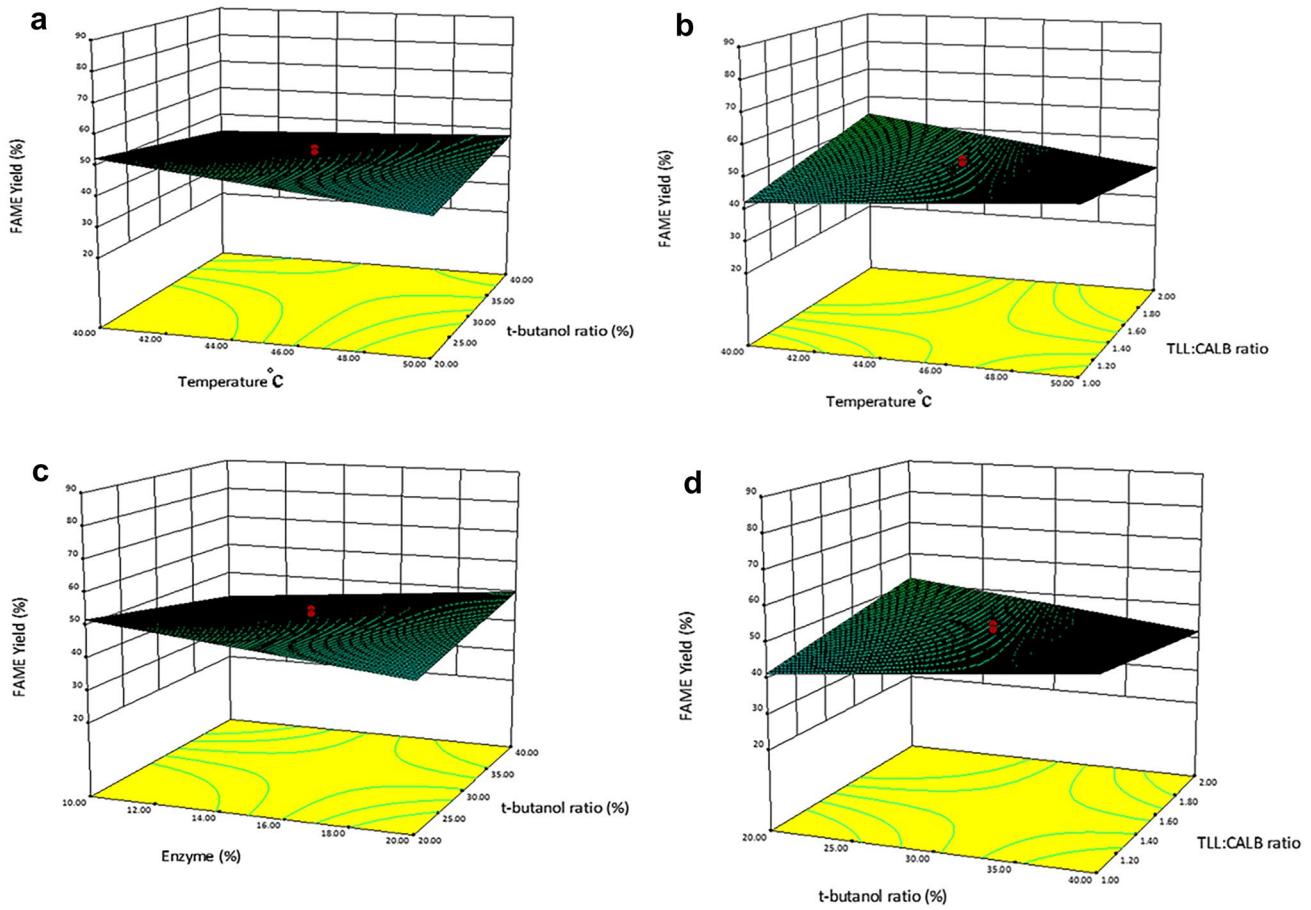

Fig. 8 Response surface plot and contour plot of FAME conversion: **a** *t*-butanol vs. temperature (°C), **b** TLL: CALB ratio vs. temperature (°C), **c** enzyme-to-oil ratio vs. *t*-butanol, and **d** TLL: CALB ratio vs. *t*-butanol

for co-immobilization and then upturns the loss of enzyme activity. Higher biodiesel production can be attributed to a decrease in mass transfer limitations due to lower viscosity of mixture compared to the solvent-free system [60]. As can be seen in Fig. 8d at the lower level of *t*-butanol by increasing the ratio of TLL:CALB, FAME production will increase from 42 to 52%.

Reusability of co-immobilized derivatives

The reusability of immobilized catalyst is an important parameter, for industrial application and minimizing costs which can determine the economic viability of any biocatalytic process. Higher reusability resulted in higher conversion, thereby lowering the biodiesel production price [61]. To investigate recyclability of the co-immobilized derivatives, they were repeatedly used in biodiesel without using *t*-butanol. After each run, the co-immobilized preparations were recovered using magnets, washed with *n*-hexane, dried, and reused five times. Figure 9 (TLL:CALB and RML:CALB) shows the heterogeneous catalyst activity after 5 reuses of immobilized enzymes.

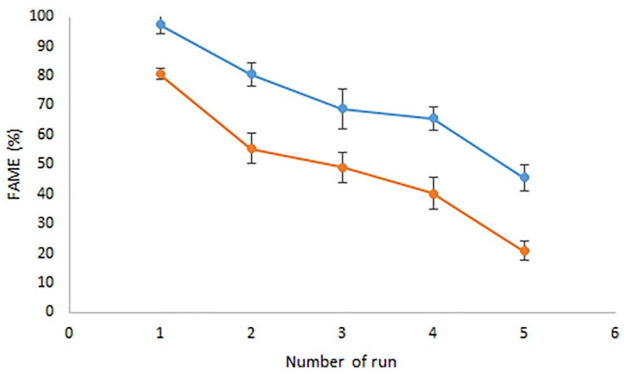

Fig. 9 The effect of repeated use of co-immobilized Fe_3O_4@SiO_2-NH_2-RML-CALB (■),Fe_3O_4@SiO_2-NH_2-TLL-CALB (●) on their activity in biodiesel production: 130 mg waste cooking oil, oil-to-methanol molar ratio of 1:3, reaction temperature 50 °C, and reaction time 24 h

The co-immobilized TLL:CALB gave 79% FAME yield after 3 run and RML:CALB reached to half of its initial yield.

Conclusions

It is demonstrated for the first time Fe_3O_4@SiO_2-NH_2 used as a support to co-immobilized RML:CALB and TLL:CALB in different ratios. The resulting immobilized preparations were also used as a biocatalyst to catalyze transesterification of waste cooking oil with methanol to produce fatty acid methyl esters (FAMEs). This immobilization procedure was performed at room temperature in water (pH 7.0) in a short time (2-7 h) without a significant decrease in the specific activity of the enzymes. The high stability of the Fe_3O_4@SiO_2-NH_2-TLL-CALB and Fe_3O_4@SiO_2-NH_2-RML-CALB was demonstrated by examination in different pH, co-solvents, and temperatures. Also, immobilized TLL:CALB and RML:CALB can retain most of their activity in wide ranges of temperatures than free enzyme. RML-CALB and TLL-CALB co-immobilized derivatives had specific activity of about 34 and 35 U/g and yield of biodiesel production were about 99 and 81%, respectively. This work presented a new approach to the production of biodiesel using a co-immobilized enzyme which gave the higher yields compared with individually immobilized enzymes.

Supplementary Information The online version contains supplementary material available at https://doi.org/10.1007/s00449-022-02808-7.

Declarations

Conflict of interest The authors declare that they have no known competing financial interests or personal relationships that could have appeared to influence the work reported in this paper.

References

1. Franssen MC, Steunenberg P, Scott EL, ZuilhofSanders H (2013) Immobilised enzymes in biorenewables production. R Soc Chem 42:6491–6533. https://doi.org/10.1039/C3CS00004D
2. Babaki M, Yousefi M, Habibi Z, MohammadiBrask M (2015) Effect of water, organic solvent and adsorbent contents on production of biodiesel fuel from canola oil catalyzed by various lipases immobilized on epoxy-functionalized silica as low cost biocatalyst. Mol Catal B: Enzym 120:93–99. https://doi.org/10.1016/j.molcatb.2015.06.014
3. Georgogianni K, Kontominas M, Tegou E, Avlonitis D, Gergis V (2007) Biodiesel production: reaction and process parameters of alkali-catalyzed transesterification of waste frying oils. Energy Fuels 21:3023–3027. https://doi.org/10.1021/ef070102b
4. Gerpen V (2005) Biodiesel processing and production. Fuel Process Technol 86:1097–1107. https://doi.org/10.1016/j.fuproc.2004.11.005
5. Haas MJ, Michalski PJ, Runyon S, Nunez A, Scott KM (2003) Production of FAME from acid oil, a by-product of vegetable oil refining. J Am Oil Chem Soc 80:97–102. https://doi.org/10.1007/s11746-003-0658-4
6. C. Wancura JH, Tres MV, Jahn SL, de Oliveira JV, (2020) Lipases in liquid formulation for biodiesel production: current status and challenges. Biotechnol Appl Biochem 67:648–667. https://doi.org/10.1002/bab.1835
7. Wancura JH, Fantinel AL, Ugalde GA, Donato FF, de Oliveira JV, Tres MV, Jahn SL (2021) Semi-continuous production of biodiesel on pilot scale via enzymatic hydroesterification of waste material: process and economics considerations. J Cleaner Prod 285:124838. https://doi.org/10.1016/j.jclepro.2020.124838
8. Wancura JH, Rosset DV, Ugalde GA, Oliveira JV, Mazutti MA, Tres MV, Jahn SL (2019) Feeding strategies of methanol and lipase on eversa® transform-mediated hydroesterification for FAME production. J Chem Eng 97:1332–1339. https://doi.org/10.1002/cjce.23404
9. Zhang B, Weng Y, Xu H, Mao Z (2012) Enzyme immobilization for biodiesel production. Appl Microbiol Biotechnol 93:61–70. https://doi.org/10.1007/s00253-011-3672-x
10. Weiser D, Nagy F, Bánóczi G, Oláh M, Farkas A, Szilágyi A, László K, Gellért Á, Marosi G, Kemény SJ (2017) Immobilization engineering–How to design advanced sol–gel systems for biocatalysis? Green Chem 19:3927–3937. https://doi.org/10.1039/C7GC00896A
11. Alamsyah G, Albels VA, Sahlan M, Hermansyah HJ (2017) Effect of chitosan's amino group in adsorption-crosslinking immobilization of lipase enzyme on resin to catalyze biodiesel synthesis. Energy Procedia 136:47–52. https://doi.org/10.1016/j.egypro.2017.10.278
12. Adlercreutz PJ (2013) Immobilisation and application of lipases in organic media. Chem Soc Rev 42:6406–6436. https://doi.org/10.1039/C3CS35446F
13. Sassolas A, Blum LJ, Leca-Bouvier BD (2012) Immobilization strategies to develop enzymatic biosensors. Biotechnol Adv 30:489–511. https://doi.org/10.1016/j.biotechadv.2011.09.003
14. Barbosa O, Torres R, Ortiz C, Berenguer-Murcia Á, Rodrigues RC, Fernandez-Lafuente R (2013) Heterofunctional supports in enzyme immobilization: from traditional immobilization protocols to opportunities in tuning enzyme properties. Biomacromol 14:2433–2462. https://doi.org/10.1021/bm400762h
15. Yildiz H, Ozyilmaz E, Bhatti AA (2017) Enantioselective resolution of racemic flurbiprofen methyl ester by lipase encapsulated mercapto calix[4]arenes capped Fe_3O_4 nanoparticles. Bioprocess Biosyst Eng 40:1189–1196. https://doi.org/10.1007/s00449-017-1779-x
16. Ozyilmaz E, Sayin S (2013) A magnetically separable biocatalyst for resolution of racemic naproxen methyl ester. Bioprocess Biosyst Eng 36:1803–1806. https://doi.org/10.1007/s00449-013-0941-3
17. Liu X (2018) Preparation of porous hollow Fe_3O_4/P(GMA–DVB–St) microspheres and application for lipase immobilization. Bioprocess Biosyst Eng 41:771–779. https://doi.org/10.1007/s00449-018-1910-7
18. Mohammadi M, Ashjari M, Dezvarei S, Yousefi M, Babaki M, Mohammadi (2015) Rapid and high-density covalent immobilization of *Rhizomucor miehei* lipase using a multi component reaction: application in biodiesel production. RSC adv 5:32698–32705. https://doi.org/10.1039/C5RA03299G
19. Mohammadi M, Ashjari M, Garmroodi M, Yousefi M, Karkhane AA (2016) The use of isocyanide-based multicomponent reaction for covalent immobilization of *Rhizomucor miehei* lipase on multiwall carbon nanotubes and graphene nanosheets. RSC adv 6:72275–72285
20. Ashjari M, Garmroodi M, Asl FA, Emampour M, Yousefi M, Lish MP, Habibi Z, Mohammadi, (2020) Application of multicomponent reaction for covalent immobilization of two lipases on aldehyde-functionalized magnetic nanoparticles; production of biodiesel from waste cooking oil. Process Biochem 90:156–167. https://doi.org/10.1016/j.procbio.2019.11.002

21. Shahedi M, Habibi Z, Yousefi M, Brask J, Mohammadi (2021) Improvement of biodiesel production from palm oil by co-immobilization of *Thermomyces lanuginosa* lipase and *Candida antarctica* lipase B: optimization using response surface methodology. Int J Biol Macromol 170:490–502. https://doi.org/10.1016/j.ijbiomac.2020.12.181
22. Sigurdardóttir SB, Lehmann J, Ovtar S, Grivel JC, Negra MD, Kaiser A, Pinelo M (2018) Enzyme immobilization on inorganic surfaces for membrane reactor applications: mass transfer challenges, enzyme leakage and reuse of materials. Adv Synth Catal 360:2578–2607. https://doi.org/10.1002/adsc.201800307
23. Vashist SK, Lam E, Hrapovic S, Male KB, Luong JH (2014) Immobilization of antibodies and enzymes on 3-aminopropyltriethoxysilane-functionalized bioanalytical platforms for biosensors and diagnostics. Chem Rev 114(21):11083–11130. https://doi.org/10.1021/cr5000943
24. Cui JD, Jia SR (2015) Optimization protocols and improved strategies of cross-linked enzyme aggregates technology: current development and future challenges. Crit Rev Biotechnol 35:15–28. https://doi.org/10.3109/07388551.2013.795516
25. Amini Y, Shahedi M, Habibi Z, Yousefi M, Ashjari M, Mohammadi M (2022) A multi-component reaction for covalent immobilization of lipases on amine-functionalized magnetic nanoparticles: production of biodiesel from waste cooking oil. Bioresour Bioprocess online published. https://doi.org/10.1186/s40643-022-00552-0
26. Alves JS, Vieira NS, Cunha AS, Silva AM, Ayub MAZ, Fernandez-Lafuente R, Rodrigues RC (2014) Combi-lipase for heterogeneous substrates: a new approach for hydrolysis of soybean oil using mixtures of biocatalysts. RSC Adv 4:6863–6868. https://doi.org/10.1039/C3RA45969A
27. Poppe JK, Matte CR, Peralba MDCR, Fernandez-Lafuente R, Rodrigues RC, Ayub MAZ (2015) Optimization of ethyl ester production from olive and palm oils using mixtures of immobilized lipases. Appl Catal A: Gen 490:50–56. https://doi.org/10.1016/j.apcata.2014.10.050
28. Ajinkya N, Yu X, Kaithal P, Luo H, Somani P, Ramakrishna S (2020) Magnetic iron oxide nanoparticle (IONP) synthesis to applications: present and future. Materials (Basel) 13:4644. https://doi.org/10.3390/ma13204644
29. Stöber W, Fink A, Bohn E (1968) Controlled growth of monodisperse silica spheres in the micron size range. J Colloid Interface Sci 26:62–69. https://doi.org/10.1016/0003-2697(76)90527-3
30. Bradford MM (1976) A rapid and sensitive method for the quantitation of microgram quantities of protein utilizing the principle of protein-dye binding. Anal Biochem 72:248–254. https://doi.org/10.1016/0003-2697(76)90527-3
31. Ahrari F, Yousefi M, Habibi Z, Mohammadi M (2022) Application of undecanedicarboxylic acid to prepare cross-linked enzymes (CLEs) of *Rhizomucor miehei* lipase (RML); Selective enrichment of polyunsaturated fatty acids. Mol Catal 520:112172. https://doi.org/10.1016/j.mcat.2022.112172
32. Basso A, Banfi L, Riva R (2011) Divergent synthesis of novel five-membered heterocyclic compounds by base-mediated rearrangement of acrylamides derived from a novel isocyanide-based multicomponent reaction. Molecules 16:8775–8787. https://doi.org/10.3390/molecules16108775
33. Mohammadi M, Gandomkar S, Habibi Z, Yousefi M (2016) One pot three-component reaction for covalent immobilization of enzymes: application of immobilized lipases for kinetic resolution of rac-ibuprofen. RSC Adv 6:52838–52849. https://doi.org/10.1039/C6RA11284F
34. Ahmadipour M, Hatami M, Rao KV (2012) Preparation and characterization of nano-sized ($Mg_{(x)}$ $Fe_{(1-x)}$ O/SiO_2)(x= 0.1) core-shell nanoparticles by chemical precipitation method. Adv Nanoparticles 1:37–43. https://doi.org/10.4236/anp.2012.13006
35. Henriques RO, Bork JA, Fernandez-Lorente G, Guisan JM, Furigo A Jr, de Oliveira D, Pessela BC (2018) Co-immobilization of lipases and β-d-galactosidase onto magnetic nanoparticle supports: biochemical characterization. Mol Catal 453:12–21. https://doi.org/10.1016/j.mcat.2018.04.022
36. Babaki M, Yousefi M, Habibi Z, Mohammadi M, Yousefi P, Mohammadi J, Brask J (2016) Enzymatic production of biodiesel using lipases immobilized on silica nanoparticles as highly reusable biocatalysts: effect of water, t-butanol and blue silica gel contents. Renew Energ 91:196–206. https://doi.org/10.1016/j.renene.2016.01.053
37. Garmroodi M, Mohammadi M, Ramazani A, Ashjari M, Mohammadi J, Sabour B, Yousefi M (2016) Covalent binding of hyperactivated *Rhizomucor miehei* lipase (RML) on hetero-functionalized siliceous supports. Int J Biol Macromol 86:208–215. https://doi.org/10.1016/j.ijbiomac.2016.01.076
38. Noureddini H, Gao X, Philkana RJ (2005) Immobilized Pseudomonas cepacia lipase for biodiesel fuel production from soybean oil. Bioresour Technol 96:769–777. https://doi.org/10.1016/j.biortech.2004.05.029Get
39. Guldhe A, Singh B, Mutanda T, Permaul K, Bux F (2015) Advances in synthesis of biodiesel via enzyme catalysis: novel and sustainable approaches. Renew Sust Energ Rev 41:1447–1464. https://doi.org/10.1016/j.rser.2014.09.035
40. Poole P, Finney JJ (1983) Hydration-induced conformational and flexibility changes in lysozyme at low water content. Int J Biol Macromol 5:308–310. https://doi.org/10.1016/0141-8130(83)90047-8
41. Jordaan J, Leukes WD (2003) Isolation of a thermostable laccase with DMAB and MBTH oxidative coupling activity from a mesophilic white rot fungus. Enzyme Microb Technol 33:212–219. https://doi.org/10.1016/S0141-0229(03)00116-9
42. Toro EC, Rodríguez DF, Morales N, García LM, Godoy CA (2019) Novel combi-lipase systems for fatty acid ethyl esters production. Catalysts 9:546. https://doi.org/10.3390/catal9060546
43. Tiosso PC, Carvalho AKF, De Castro HF, de Moraes FD, Zanin GM (2014) Utilization of immobilized lipases as catalysts in the transesterification of non-edible vegetable oils with ethanol. Braz J Chem Eng 31:839–847. https://doi.org/10.1590/0104-6632.20140314s00003006
44. Peng B, Yang JY, Liu X, Hu JN, Zheng LF, Li J, Deng ZY (2020) Enzymatic synthesis of 1, 3-oleic-2-medium chain triacylglycerols and strategy of controlling acyl migration: insights from experiment and molecular dynamics simulation. Int J Food Prop 23:1082–1096. https://doi.org/10.1080/10942912.2020.1775645
45. Peng B, Chen F, Liu X, Hu JN, Zheng LF, Li J, Deng ZY (2020) Trace water activity could improve the formation of 1, 3-oleic-2-medium chain-rich triacylglycerols by promoting acyl migration in the lipase RM IM catalyzed interesterification. Food Chem 313:126130. https://doi.org/10.1016/j.foodchem.2019.126130
46. Pacheco C, Crapiste GH, Carrín ME (2015) Study of acyl migration during enzymatic interesterification of liquid and fully hydrogenated soybean oil. J Mol Catal B Enzym 122:117–124. https://doi.org/10.1016/j.molcatb.2015.08.023
47. Binhayeeding N, Klomklao S, Prasertsan P, Sangkharak K (2020) Improvement of biodiesel production using waste cooking oil and applying single and mixed immobilised lipases on polyhydroxyalkanoate. Renew Energy 162:1819–1827. https://doi.org/10.1016/j.renene.2020.10.009
48. Yasvanthrajan N, Sivakumar P, Muthukumar K, Murugesan T, Arunagiri A (2021) Production of biodiesel from waste bio-oil through ultrasound assisted transesterification using immobilized lipase. Environ Technol Innov 21:101199. https://doi.org/10.1016/j.eti.2020.101199
49. Wenlei X, Huang M (2020) Fabrication of immobilized Candida rugosa lipase on magnetic Fe_3O_4-poly (glycidyl

methacrylate-co-methacrylic acid) composite as an efficient and recyclable biocatalyst for enzymatic production of biodiesel. Renew Energy 158:474–486. https://doi.org/10.1016/j.renene.2020.05.172
50. Wenlei X, Huang M (2018) Immobilization of Candida rugosa lipase onto graphene oxide Fe3O4 nanocomposite: characterization and application for biodiesel production. Energy Convrs Manag 159:42–53. https://doi.org/10.1016/j.enconman.2018.01.021
51. Wenlei X, Wang J (2012) Immobilized lipase on magnetic chitosan microspheres for transesterification of soybean oil. Biomass Bioenergy 36:373–380. https://doi.org/10.1016/j.biombioe.2011.11.006
52. Zhang H, Liu T, Zhu Y, Hong L, Li T, Wang X, Fu Y (2020) Lipases immobilized on the modified polyporous magnetic cellulose support as an efficient and recyclable catalyst for biodiesel production from yellow horn seed oil. Renew Energy 145:1246–1254. https://doi.org/10.1016/j.renene.2019.06.031
53. Shomal R, Du W, Al-Zuhair S (2022) Immobilization of lipase on metal-organic frameworks for biodiesel production. J Environ Chem Eng 10:107265. https://doi.org/10.1016/j.jece.2022.107265
54. Rafiei S, Tangestaninejad S, Horcajada P, Moghadam M, Mirkhani V, Mohammadpoor-Baltork I, Kardanpour R, Zadehahmadi F (2018) Efficient biodiesel production using a lipase@ ZIF-67 nanobioreactor. Chem Eng J 334:1233–1241. https://doi.org/10.1016/j.cej.2017.10.094
55. Kumar R, Pal P (2021) Lipase immobilized graphene oxide biocatalyst assisted enzymatic transesterification of Pongamia pinnata (Karanja) oil and downstream enrichment of biodiesel by solar-driven direct contact membrane distillation followed by ultrafiltration. Fuel Process Technol 211:106577. https://doi.org/10.1016/j.fuproc.2020.106577
56. Li Q, Zheng J, Yan YJ (2010) Biodiesel preparation catalyzed by compound-lipase in co-solvent. Fuel Process Technol 91:1229–1234. https://doi.org/10.1016/j.fuproc.2010.04.002
57. Klibanov AM (1989) Enzymatic catalysis in anhydrous organic solvents. Trends Biochem Sci 14:141–144. https://doi.org/10.1016/0968-0004(89)90146-1
58. Du W, Liu D, Li L, Dai L (2007) Mechanism exploration during lipase-mediated methanolysis of renewable oils for biodiesel production in a tert-butanol system. Biotechnol Prog 23:1087–1090. https://doi.org/10.1021/bp070073n
59. Arana-Peña S, Carballares D, Berenguer-Murcia Á, Alcántara AR, Rodrigues RC, Fernandez-Lafuente R (2020) One pot use of combilipases for full modification of oils and fats: multifunctional and heterogeneous substrates. Catalysts 10:605–662. https://doi.org/10.3390/catal10060605
60. Sim JH, Kamaruddin AH, Bhatia S (2010) The feasibility study of crude palm oil transesterification at 30 °C operation. Bioresour Technol 101:8948–8954. https://doi.org/10.1016/j.biortech.2010.07.039
61. Fjerbaek L, Christensen KV, Norddahl B (2009) A review of the current state of biodiesel production using enzymatic transesterification. Biotechnol Bioeng 102:1298–1315. https://doi.org/10.1039/C3CS00004D